

## THE EFFECTS OF FRICTION COEFFICIENT AND INTERFERENCE ON THE FRETTING FATIGUE STRENGTH OF RAILWAY AXLE ASSEMBLY

Mohammad ZEHSAZ<sup>1</sup>, Pouya SHAHRIARY<sup>2</sup>

*In railway transportation, the press-fit of wheel and axle are one of the most critical components for railway vehicle with regard to safety. Fretting fatigue can occur in press-fitted shafts subjected to rotating bending such as railway axles. Cyclic stress and micro slippage between shaft and hub are the main causes of fretting fatigue, which reduces the fatigue strength of axle considerably. Friction coefficient and interference have an important effect on fretting fatigue. In this paper contact stresses were extracted along a longitudinal path at the top surface of the shaft through finite element method. Then the effects of coefficient of friction and interference on fretting fatigue strength of railway axles are studied using fretting damage parameters (Ruiz- Chen parameters). Results demonstrate that by increasing the friction coefficient and interference the fretting fatigue strength of the axle decreases.*

**Keywords:** Fretting Fatigue, Railway Axle, Friction Coefficient, Interference

### 1. Introduction

Railway axle is one of the most important components of railway vehicles, since it is subjected to rotating bending and the issue of fatigue failure always exists. Fretting fatigue is a typical high cycle fatigue due to the cyclic minute relative slip between the axle surface and the inner surface of wheel hub, which initiates micro cracks and wear (1998) [1]. When the fretting occurs in the press-fitted shaft, the fatigue strength remarkably decreases compared to that of without fretting (1972) [2].

Considering the importance of railway axles and in order to maintain the safety of axles, many investigations and experiments have been carried out by researchers ever since. Hoger (1952) [3] reported various factors influencing fatigue strength of press-fitted assemblies such as clamping pressure, shape or geometry of assembly. Nishioka and Komatsu (1969, 1972) [4, 5] attempted to increase the fatigue limits of press-fitted specimens by changing the geometry of

<sup>1</sup> Associated Professor, Dept.of Mechanical Engineering, Tabriz University, Iran, e-mail: zehsaz@tabrizu.ac.ir

<sup>2</sup> Ms student, Dept.of Mechanical Engineering, Tabriz University, Iran, e-mail: p.shahriari89@ms.tabrizu.ac.ir

press-fitted portion. *Kubota et al.* (2003) [6] tried to clarify the effect of under stress on fretting fatigue crack initiation behavior in the press-fitted axles.

By the progress of numerical methods and advances in computer programs, studying the fretting fatigue came to new stage. Finite element methods used to calculate different parameters to predict fretting fatigue. *Lykins et al.* (2000) [7] evaluated how well some of fatigue parameters predict fretting fatigue crack initiation using finite element method. *Ekberg* (2004) [8] provided an overview of different types of numerical models available to predict fretting fatigue and outlined a numerical model for analysis of fretting fatigue in a finite element simulation of the assembly. *Vinder and Leidich* [9] in 2009 introduced new energy-based approach for predicting fretting fatigue and applied it for key-shaft-hub connections. *Alfredsson* (2009)[10] simulated the fretting fatigue phenomena in a shrink-fit pin subjected to rotating bending using finite element method, and studied the risk of fretting fatigue by the means of two fretting fatigue criteria. In 2011 *Lanoue et al.* [11] calculated fretting fatigue strength reduction factor for interference fits based on a comparison between experimental data and finite element analysis for many configurations of interference fits in rotating bending and alternated torsion.

However, in the railway axle, the problems of the fretting fatigue crack initiation at press-fitted axle parts have not been completely solved [1] and the study on the mechanism of fretting crack nucleation is necessary for improvement of fatigue strength and for determination of period of regular overhaul inspection to ensure safety. In this paper, fretting fatigue damage parameters (Ruiz- Chen parameters) have been used for studying the effect of friction coefficient and interference on fretting fatigue strength of railway axles.

## 2. Finite element simulation

The finite element analysis of railway axle has been carried out by employing the computer code ANSYS. The observed railway axle has been designed for 200 kN axial load based on UIC<sup>1</sup> standard method. The diameter of wheel seat is 185 mm and the diameter of wheel hub is 1000 mm, also the axle body diameter is 160 mm and the length of the axle is 2156 mm [12].

In order to utilize the finite element analysis a meshed model of the wheel hub and axle should be developed in the finite element software. Solid185 elements have been used for meshing the axle and the wheel hub. These elements have 8 nodes and 3 degrees of freedom at each node. They can include plasticity, stress stiffening and large deflections in the model and they are also suitable for nonlinear analysis [13].

---

<sup>1</sup> International Union of Railways

Contact174 and Target173 elements have been engaged for modeling the contact between axle and wheel hub. These contact elements allow pressure to be transferred between the contacting surfaces but prevent penetration with each other. They can also measure the micro slippage between contact surfaces [13].

Considering the nonlinearity of the equations on the contact surface and the necessity of the convergence of the calculations, the Augmented Lagrangian contact algorithm has been used in simulations [14].

After finite element modeling and analyzing the problem with different element sizes, the appropriate element size has been chosen considering the convergence of the problem and the accuracy of the calculations. In the final model, there have been 50624 solid elements and 5248 contact elements in the model with a higher density close to the contact edge where high stress gradients were expected. The finite element model of final assembly is shown in Fig.1.

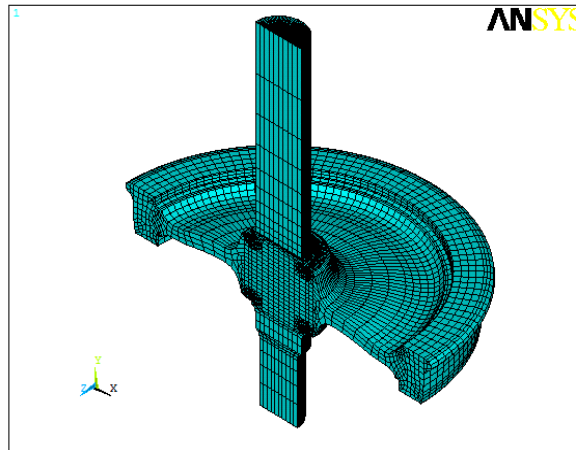


Fig. 1. Mesh for the assembly model

## 2.1. Boundary conditions

Railway axles are subjected to rotating bending due to the weight of the train. The weight force acts on the axle through bearing journals and the track acts as a support for the wheel. Fig.2 shows the scheme of the load and the consequent bending moment on the axle.

Due to the symmetric condition of the load in respect to the axle geometry (centre line of it), the quarter model of the axle has been used for the study and the symmetric boundary conditions have been applied on the symmetry planes. Boundary conditions are presented in Fig.3.

The analysis was split into two steps, first step was applying interference fit and the second step was applying the load. Spring elements were used for

stabilizing the solution. The stiffness of the spring elements was set to 1 N/mm which is a value without physical meaning.

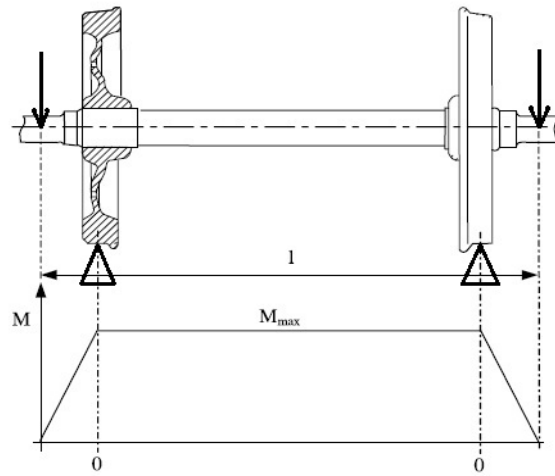


Fig. 2. Scheme of loading and the consequent bending moment on the axle

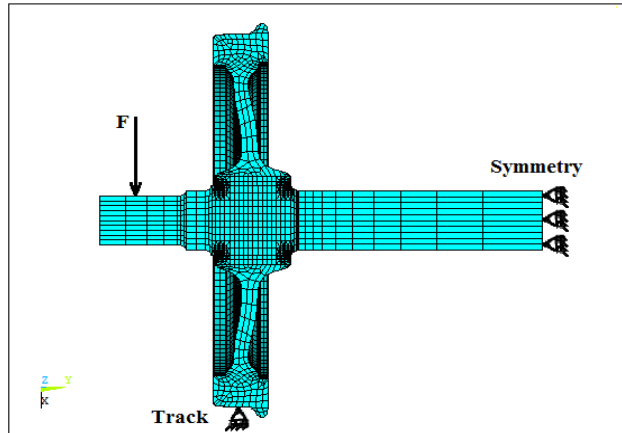


Fig. 3. Used boundary conditions on the axle

In order to study the fretting fatigue strength of the axle on the contact surface, the origin of the local coordinate system is located on the centre of the contact area. Fig.4 shows the local coordinate system on the contact surface,  $r$  is the half of the length of contact area and the  $(x/r)$  shows the relative distance from contact center.

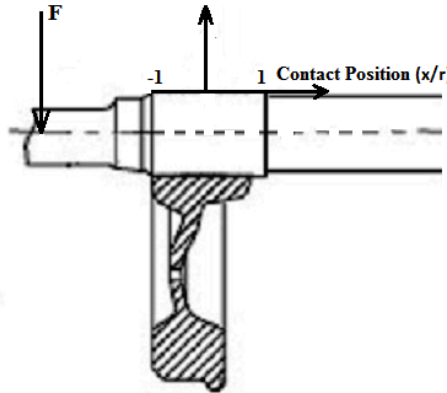


Fig. 4. Local coordinate system on the contact surface

## 2.2. Material properties

According to the UIC standard the suitable material for railway axles is A1N steel grade and the suitable material for the wheel hub is R7T steel grade [16,17]. Chemical composition and mechanical properties of the steels are in Tables.1 and 2.

Table 1

Chemical compositions of steels (wt%) [16, 17]

Steel Grade	C	Si	Mn	P	S	Cr	Mo	Cu	V	Ni
A1N	0.37	0.46	1.12	0.04	0.04	0.3	0.05	0.3	0.05	0.3
R7T	0.52	0.4	0.8	0.04	0.04	0.3	0.08	0.3	0.05	0.3

Table 2

Mechanical properties of A1N and R7T steels [16, 17]

Steel Grade	S <sub>y</sub> (MPa)	S <sub>ut</sub> (MPa)	Elongation (%)	Minimum impact energy at 20°C (J)
A1N	320	550-650	22	25
R7T	560	820-940	14	15

An elastic-plastic material formulation has been chosen in numerical simulations, to improve the local stress and strain calculations, especially avoiding overestimations of local wear distributions.

## 3. Interference fit

Press fitting and shrink fitting are two methods of attaching the wheel hub to the axle. In order to have a right attachment, UIC code sets a restriction for the proportion of the interference [15]. The maximum and minimum allowable values of the radial interference are presented in equations (1) and (2).

$$2v_{max} = 0.0015D + 0.06 \quad (1)$$

$$2v_{min} = 0.0009D \quad (2)$$

In these equations  $v$  and  $D$  are the radial interference and diameter of the wheel seat respectively. The dimensions are in millimeters.

#### 4. Fretting parameters

Fretting occurs between components that are together in contact and undergo a small amplitude cyclic-type loading that causes them to have at least some small tangential displacement relative to each other. When the presence of fretting is associated with decreased fatigue performance, such as shorter life, the effect is called fretting fatigue. Ruiz et al. [18] have proposed a fretting parameter, based on work energy principles. They realized that the work performed in fretting is the local shear stress times the local displacement.

$$F_1 = \tau\delta \quad (3)$$

This parameter is known as the fretting wear parameter. Here  $\tau$  is the interfacial shearing stress, which can be created due to the friction between contact areas,  $\delta$  is relative slip between contact surfaces and  $F_1$  represents the friction work per unit area.  $F_1$  has been shown to be fairly accurate in predicting nucleation sites and it is directly related to the depth of the wear scar.

Ruiz and Chen empirically added the maximum normal stress to  $F_1$  and introduced fretting fatigue parameter  $F_2$  to account for global bending of the fretted specimen [19]. The factors involved in fretting parameters are shown in Fig.5.

$$F_2 = \sigma\tau\delta \quad (4)$$

This parameter is known as the fretting fatigue parameter ( $F_2$ ) and it has been shown to be inversely related to the cyclic life. Here  $\sigma$  is the tension acting parallel to contact surface. Furthermore; Lykins et al. [7] state that it predicts the locations for crack initiation well.

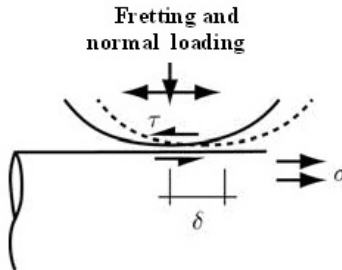


Fig. 5. Factors involved in fretting parameters [7]

## 5. Results

The fretting fatigue strength of railway axle has been studied in different combinations of the friction coefficient and interference. Friction coefficient and interference in each case have been presented in Table.3. From the finite element assembly model the contact stresses were extracted along a longitudinal path at the top surface of the shaft. In the following, obtained results will be discussed.

### 5.1. Slip region

The relative slip region has been determined in each case and the results are presented in Table.3. For partial slip conditions, the slip region is identified as the part of the contact where frictional shear traction,  $q(x)$ , is equal to the contact pressure times the coefficient of friction,  $\mu p(x)$ , ( $c/r$ ) shows the relative sliding distance from the contact center. In Fig.6 frictional shear traction,  $q(x)$ , is plotted together with the contact pressure times the coefficient of friction,  $\mu p(x)$ , for friction coefficient of  $\mu = 0.2$  and some interferences (in micrometers).

According to the results in Table.3, it is clear that when interference and pressure are increased, the shear traction increases and the distance with relative slip decreases. In other words starting location of the slip region transmits towards the contact edge by increasing the interference. The same behavior happens by increasing the coefficient of friction.

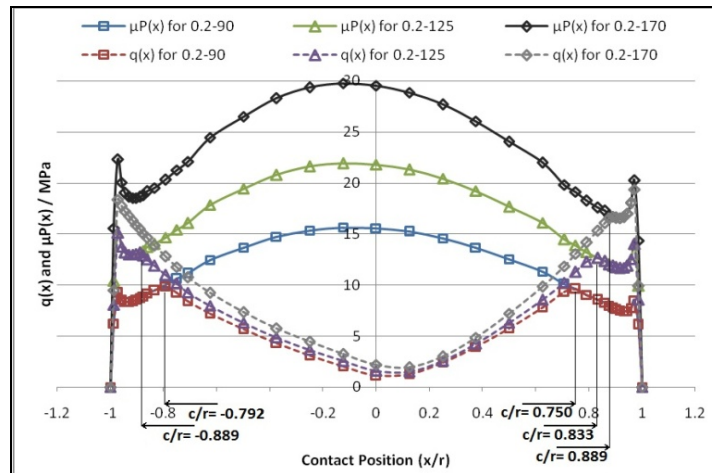


Fig. 6. Pressures, shear tractions along the top side of the shaft for some radial interference and  $\mu=0.2$ .

Table 3

Results of friction coefficient and interference in each case

Coefficient of Friction	Radial Interference $v$ ( $\mu\text{m}$ )	Relative Sliding Distance ( $c/r$ )	$F_1$ max (MPa.mm)	$F_2$ max (MPa $^2$ .mm)
0.1	90	-0.708	0.625	0.125
0.1	125	-0.792	0.708	0.210
0.1	150	-0.833	0.750	0.282
0.1	170	-0.861	0.792	0.344
0.2	90	-0.792	0.750	0.165
0.2	125	-0.889	0.833	0.297
0.2	150	-0.986	0.861	0.400
0.2	170	-	0.889	0.473
0.4	90	-0.916	0.861	0.208
0.4	125	-0.986	0.944	0.328
0.4	150	-0.986	0.986	0.423
0.4	170	-	0.986	0.494
0.6	90	-0.958	0.931	0.195
0.6	125	-	-	-
0.6	150	-	-	-
0.6	170	-	-	-

In some cases, due to the high contact pressure and high friction coefficient, frictional shear traction does not reach the amount of contact pressure times the coefficient of friction and as a result relative slip between axle and wheel does not occur. As it is presented in Fig.6, in the case of  $\mu=0.2$  and  $v=170$  ( $\mu\text{m}$ ), sliding does not occur at outer positions of the contact area ( $x/r < 0$ ).

It is evident that if there is no relative slip between the axle and hub, fretting fatigue would not take place. Therefore, determination of fretting fatigue parameters is pointless.

## 5.2. $F_1$ parameter

Taking into account the multitude of results, the diagrams of the  $F_1$  parameter for different interferences are presented for each coefficient of friction (Figs. 7 up to 9).

According to the figures, it is evident that the fretting wear parameter ( $F_1$ ) is maximum at the contact edges which results in a deeper wear scar there. This might be due to higher friction traction ( $\tau$ ) at contact edges and higher relative slip

amplitude. Moreover, by increasing the interference, the contact pressure and consequently the friction traction at contact edges increase which results to higher fretting wear parameter. The same effect takes place by increasing the friction coefficient at a specific radial interference. This might be also because of higher friction traction. On the other hand, decreasing the coefficient of friction increases the slip amplitude as it has been presented in Fig.10. Therefore deeper fretting wear scar might be expected by decreasing friction coefficient [20] but as the figures represent, the fretting wear scar decreases by decreasing the coefficient of friction which might be due to the effect of friction traction.

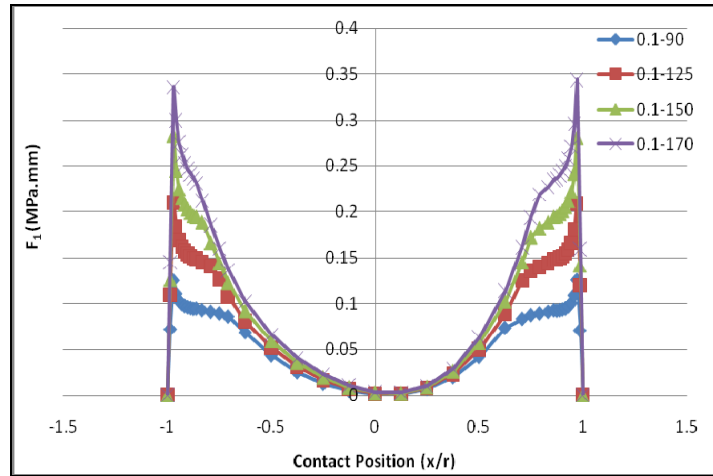


Fig. 7. Fretting wear parameter in the case of  $\mu=0.1$  and different interferences

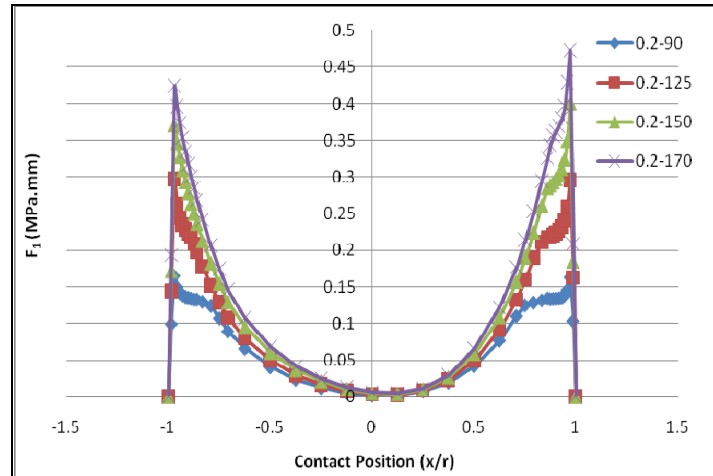


Fig. 8. Fretting wear parameter in the case of  $\mu=0.2$  and different interferences

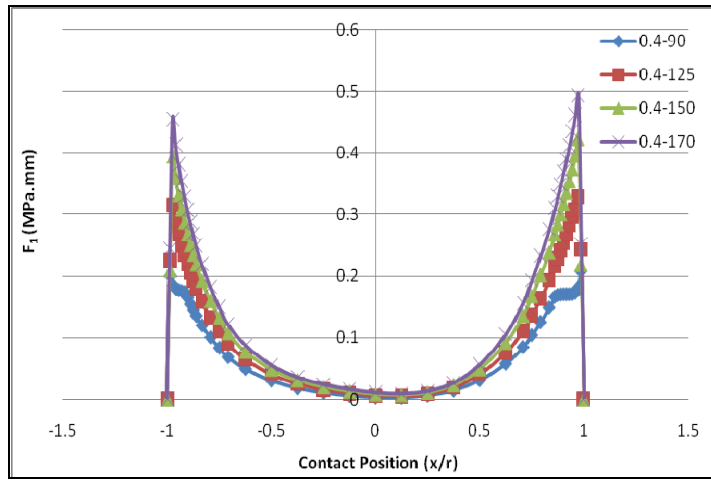


Fig. 9. Fretting wear parameter in the case of  $\mu=0.4$  and different interferences

### 5.3. $F_2$ parameter

Diagrams of the  $F_2$  parameter for different interferences are presented at each coefficient of friction (Figs.11 up to 13). Due to the press fit, the wheel squeezes the axle under its seat and stretches the surrounding regions. In other words, when interference is applied between wheel hub and axle, compressive axial stresses are caused on most parts of the contact surface. However; due to the fillet on the wheel hub, axial stresses caused by interference fit are in tension mode at contact edges. The corresponding longitudinal stress field is represented by the contours given in Fig.14.

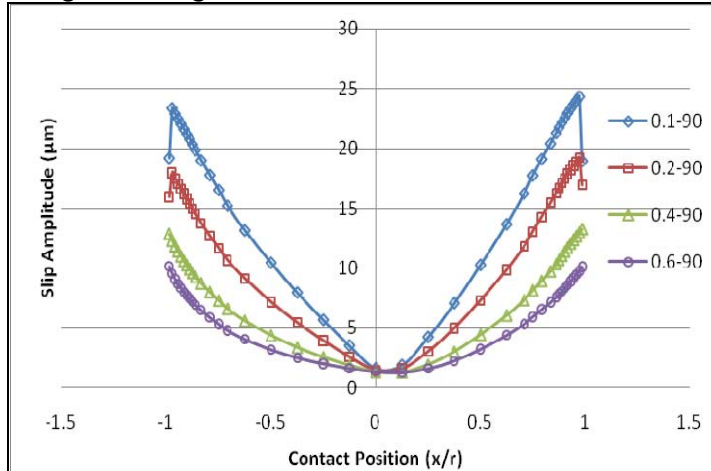


Fig.10. Slip amplitude at  $v=90$  ( $\mu\text{m}$ ) and different friction coefficient

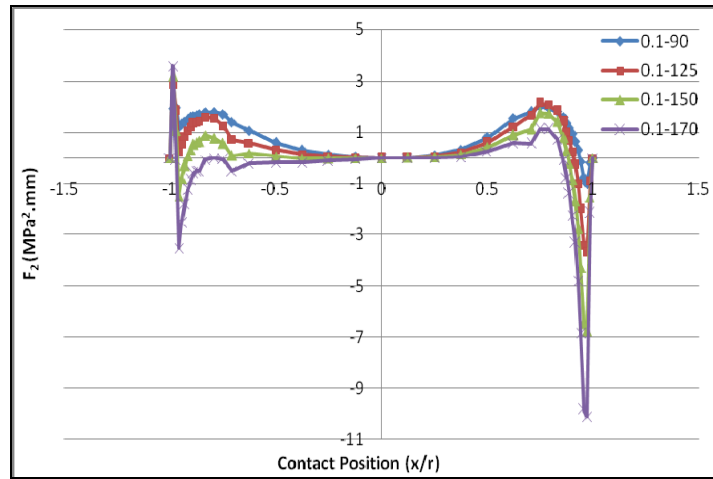


Fig.11. Fretting fatigue damage parameter in the case of  $\mu=0.1$  and different interferences

By increasing the radial interference the magnitude of the compressive stresses increase and consequently by applying the bending loads on the axle, the resulting stresses on the contact surface are decreased. On the other hand, increasing the interference intensifies tensile stresses and fretting damage at contact edges. Fig.15 shows the distribution of axial stress on contact surface due to the interference fit and bending load at different interferences. According to what has been said, an optimum amount should be considered for radial interference.

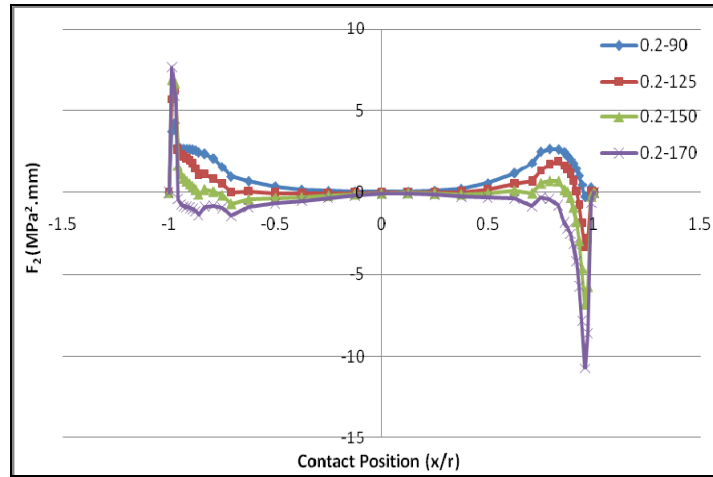


Fig.12. Fretting fatigue damage parameter in the case of  $\mu=0.2$  and different interferences

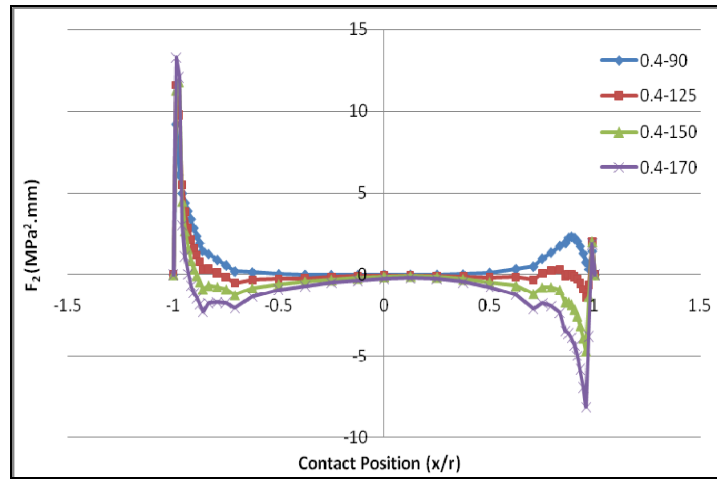


Fig.13. Fretting fatigue damage parameter in the case of  $\mu=0.4$  and different interferences

Considering that  $F_2$  parameter results from  $F_1$  parameter times the axial tensile stress, the increase of  $F_1$  parameter due to the higher friction coefficient causes the fretting fatigue parameter ( $F_2$ ) to increase and reduces the fretting fatigue strength of the axle.

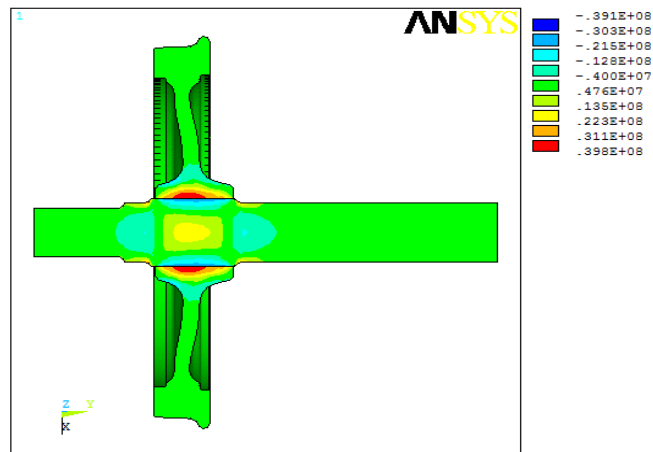


Fig.14. Longitudinal stress field induced by interference fit at  $v=125$  ( $\mu\text{m}$ )

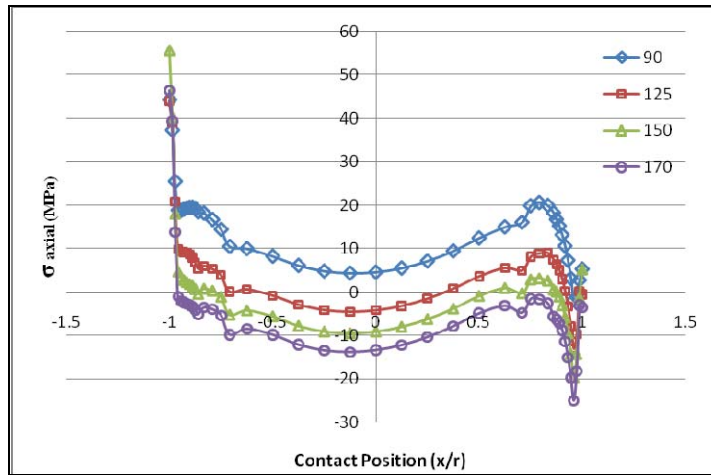


Fig.15. Axial stress in different interferences

## 6. Conclusion

The obtained results demonstrate that relative slip between wheel hub and axle occur in the areas where frictional shear traction,  $q(x)$ , is equal to the contact pressure times the coefficient of friction,  $\mu p(x)$ . By increasing the interference fit and friction coefficient the slip region transfers to the contact edges.

In the places where micro slippage occur the fretting wear parameter has the maximum amount in comparison to the other contact areas. Moreover; the friction coefficient and radial interference are in direct proportion with fretting wear damage. It has been accepted that higher slip amplitude has harmful effect on fretting wear. Although increasing the friction coefficient reduces the slip amplitude, it intensifies the fretting wear damage due to the increase of friction traction. It demonstrates that friction traction is more effective on fretting wear than slip amplitude.

Due to the fillet on the wheel hub, axial stresses caused by interference fit are in tension mode at contact edges. Thus, increasing the interference intensifies tensile stresses and fretting damage at contact edges. Furthermore, intensification of the fretting wear by increment of friction coefficient increases the fretting fatigue damage parameter ( $F_2$ ).

## R E F E R E N C E S

- [1] *K. Hirakawa, K. Toyama and M. Kubota. "The analysis and prevention of failure in railway axles", Int. J. Fatigue, Vol. 20, No. 2, 1998, pp.135-144.*
- [2] *R.B. Waterhouse, FRETTING CORROSION, Pergamon Press, Oxford 1972.*

- [3] *O.J. Hoger*."Influence of fretting corrosion on the fatigue strength of fitted members", ASTM STP144 (1952), pp. 40-51.
- [4] *K. Nishioka et al.*."Researches on increasing the fatigue strength of press-fit shaft", Bull Of JSME. **Vol.15**, No.87,1972, pp1019-1028
- [5] *K. Nishioka and K. Hirakawa*. "Fundamental investigations of fretting fatigue (Part 3. Some Phenomena and Mechanics of Surface Cracks)", Bull. Of JSME, **Vol. 12**, No. 51, 1969, pp. 397-407.
- [6] *M. Kubota, S. Niho, C. Sakae, Y. Kondo*, "Effect of understress on fretting fatigue crack initiation of press-fitted axle", Int. J. JSME, **Vol 46** , 2003, pp. 297-302.
- [7] *D. lykins, S. Mall, V. Jain*. "An evaluation of parameters for predicting fretting fatigue crack initiation", Int. J. Fatigue **Vol. 22**, 2000, pp.703-716.
- [8] *A. Ekberg*."Fretting fatigue of railway axles – a review of predictive methods and an outline of a finite element model", Proceedings of the Institution of Mechanical Engineers, Part F: Journal of Rail and Rapid Transit, **Vol. 218**, 2004, pp. 299–316.
- [9] *J. Vinder, E. Leidich*."Enhanced Ruiz criterion for the evaluation of crack initiation in contact subjected to fretting fatigue", Int. J. Fatigue **Vol. 29**, 2007, pp.2040-2049.
- [10] *B. Alfredsson*."Fretting fatigue of a shrink-fit pin subjected to rotating bending: Experiments and simulations", Int. J. Fatigue, **Vol. 31**, 2009, pp.559-1570.
- [11] *F. Lanoue, A. Vadean, B. Sanschagrin*, "Fretting fatigue strength reduction factor for interference fits", Simulation Modelling Practice and Theory, **Vol. 19**, 2011, pp.1811-1823.
- [12] UIC code 510-2, Trailing Stock: wheels and wheel set Conditions concerning, The use of wheels of various diameters, 2004.
- [13] ANSYS User's Manual for Revision 13, Copyright 2010 SAS IP, Inc. All rights reserved.
- [14] *F. Lanoue, A. Vadean, B. Sanschagrin*."Finite element analysis and contact modeling considerations of interference fits for fretting fatigue strength calculations", Simulation Modelling Practice and Theory, **Vol. 17**, 2009, pp. 1587-1602.
- [15] UIC code 813, Technical specification for the supply of wheel sets for tractive and trailing stock - Tolerances and assembly, 2nd edition, December 2003.
- [16] UIC code 811-1 OR: Technical specification for supply of axles for tractive and trailing stock, 1994.
- [17] UIC code 812-3 OR: Technical specification for the supply of solid (monobloc) wheels in rolled non-alloy steel for tractive and trailing stock,5th edition, 1984.
- [18] *C. Ruiz, P. H. B. Buddington, K. C. Chen*."An investigation of fatigue and fretting in a dovetail joint", Expl Mechanics, **Vol. 24**, 1984, pp.208-217.
- [19] *C. Ruiz, K. C. Chen*. "Life assessment of dovetail joints between blades of discs in aero-engines". Proc, Int. conf, Fatigue, Sheffield. Institute for mechanical engineers, London 1986, pp.187-194.
- [20] *GM. Spink*."Fretting fatigue of a 2<sub>1/2</sub> % Ni/Cr/Mo/V low pressure turbine steel – the effect of different contact pad materials and of variable slip amplitude", Wear, (1990), pp.81-297